Surprising Ru Capping Effects on the Spin and Orbital Magnetic Properties of CoFeB/MgO Interfaces Investigated by Synchrotron-based X-Ray Absorption Spectroscopy and X-Ray Magnetic Circular Dichroism

ANG WAN TENG, ROSLYN

(A0099393L)

NATIONAL UNIVERSITY OF SINGAPORE

2016

SURPRISING Ru CAPPING EFFECTS ON THE SPIN AND ORBITAL MAGNETIC PROPERTIES OF CoFeB/MgO INTERFACES INVESTIGATED BY SYNCHROTRON-BASED X-RAY ABSORPTION SPECTROSCOPY AND X-RAY MAGNETIC CIRCULAR DICHROISM

Ang Wan Teng, Roslyn

(A0099393L)

(*Department of Physics*)

A THESIS SUBMITTED

FOR THE DEGREE OF B.SC. (HONS.)

DEPARTMENT OF PHYSICS

NATIONAL UNIVERSITY OF SINGAPORE

2016

DECLARATION

I hereby declare that the thesis is my original work and it has been written by me in its entirety. I have duly acknowledged all the sources of information which have been used in the thesis.

This thesis has also not been submitted for any degree in any university previously.

Ang Wan Teng, Roslyn

(A0099393L)

7th April 2016

Acknowledgment

The completion of this project, albeit just the tip of the iceberg of what could potentially be an extensive study revealing ground-breaking new Physics, would not have been possible without the guidance of my supervisor Assistant Professor Andrivo Rusydi and co-supervisor Dr. Yu Xiaojiang. I would also like to thank Mr. Chi Xiao for his help with software installation, and Mr. Jason Lim for assisting with the many meetings at the Singapore Synchrotron Light Source (SSLS). Last but not least, my pizza buddies for their advise throughout the course of this project: Ng Yi'en, Tan Tu Guang, Jeremy Soh, and especially Lai Jun Hao for the discussions on the use of X-ray sum rules and help with document formatting.

Contents

Abstract

This thesis reports XAS and XMCD measurements at the $L_{2,3}$ edge of Co and Fe and magnetic moment calculations of CoFeB/MgO systems, with and without a 1nm Ru capping layer. XAS and XMCD measurements reveal multiplet effects in Fe and inversion of Co XMCD upon addition of a capping layer. Also, spin and orbital magnetic moment calculations using x-ray sum rules reveal negative magnetic moments for Co after capping addition, suggesting a flip in spin. Since no oxygen was found in the CoFeB layer, and the flip was element specific, it was proposed that this phenomenon was the consequence of Ru charge transfer across the MgO layer to interface Fe, and spin-orbit coupling between Fe and Co.

Chapter 1

Foreword

This report documents the student's journey to analyse X-ray absorption spectroscopy (XAS) and X-ray magnetic circular dichroism (XMCD) data of CoFeB/MgO interface systems. XAS and XMCD data was analyzed using knowledge gained by the student on these 2 methods during the course of this project. The use of the X-ray sum rule was also verified by reproducing literature values, to ensure correct usage of the sum rule. As this project was a collaboration between the Singapore Synchrotron Light Source (SSLS) and A*STAR Data Storage Institute (DSI), some details concerning the methodology and structural analysis (e.g. EELS) of the 2 samples fabricated by DSI were kept confidential and not available to the author. All information about the samples' fabrication and structure reported was all that was made known to the author, and the analysis of the samples were based on that. Also, due to the time constraints of this project, data from only 2 samples were provided by the supervisor. The author suggests that more research should be done for more in-depth analysis of the oxide interface's magnetic properties, and proposes several areas of further research.

Chapter 2

Introduction

Due to its potential for use in spin-transfer-torque magnetoresistive random access memory (STT-MRAM), the magnetic properties of CoFeB/MgO-based systems have been of much interest in recent times [1]. In particular, the CoFeB/MgO interface has been found to exhibit high tunnel magnetoresistance (TMR) and perpendicular magnetic anisotropy (PMA)[2, 3, 4], even higher than the PMA of traditional ferromagnetic or ferrimagnetic metals on non-magnetic transition metals [5, 6]. As several magnetic phenomena can be attributed to spin-orbit interaction (SOI)[7, 8, 9], it is believed that the control of SOI strength of interface materials is thus the key to improving the magnetic and charge transport properties of current spintronic devices, pushing the frontier of data storage devices[10]. However, while it is well known that the CoFeB/MgO interface experiences magnetic anisotropy, the role of oxygen at the interface and the origin of such anisotropy at the interface remains unclear. Furthermore, the effects of a capping layer on the interface of interest has yet to be studied extensively, and remains a crucial area of research considering the CoFeB/MgO interface's application in data storage devices.

The aim of this project was to investigate the above-mentioned problem using synchrotron-based X-ray absorption spectroscopy (XAS) and X-ray

magnetic circular dichroism (XMCD) at the $L_{2,3}$ edges of cobalt (Co) and iron (Fe).

2.1 Background knowledge

2.1.1 Interface versus bulk properties

A solid interface comprises of the few atomic layers, which separate two solids in contact with one another, with properties significantly different from those of the bulk materials it separates [11]. Since the interface lies inside the sample, and has properties dependent on its morphology after fabrication, one cannot use destructive methods of analysis that might affect the morphology of the material. Also, unlike surface properties that can be measured by using probes that interact mainly with the top few layers of atoms (e.g. low energy electron diffraction (LEED), atomic force microscopy (AFM))[11], interfaces require probes that can penetrate into the material and interact with the interface. Consequently, thin film systems (where each material layer's thickness is on the scale of nanometers) are used to study interfaces as bulk effects are reduced, allowing penetrating probes (e.g. X-rays) to be largely affected by the interface properties instead.

At an interface between two different materials, the amount change the interface atoms experience relative to their intrinsic bulk properties is largely dependent on the choice of materials (inclusive of substrate and any buffer layers) and preparation technique[11]. It is thus important to have a clear understanding of how to isolate each element's behaviour at the interface, as well as have knowledge of the film morphology through non-destructive analysis techniques (or by choosing fabrication methods with predictable results).

2.1.2 Spin and Orbital magnetic moment

Classically, magnetic moment, more correctly magnetic dipole moment, is a property of an object that governs its own magnetic field and its response when placed in a magnetic field[12]. However, the quantities to be calculated in this experiment, m_{orb} and m_{spin} although also called the the orbital and spin magnetic moment quantum numbers respectively, are actually misnomers[13]. In quantum physics, m first appears as a variable inside the spherical harmonics, used as a solution to finding the eigenvalues of the angular momentum operators L^2 and L_z, where L_z is the angular momentum in a particular direction.

$$\begin{aligned} \mathbf{L}^2 Y_l^m(\theta,\phi) &= l(l+1)\hbar^2 Y_l^m(\theta,\phi) \\ \mathbf{L}_z Y_l^m(\theta,\phi) &= m\hbar Y_l^m(\theta,\phi) \end{aligned} \tag{2.1}$$

As shown in (2.1), m is the eigenvalue of L_z, implying that m is a directional quantum number. Later, due to experimental evidence (Zeeman effect and Stern-Gerlach experiment), it was postulated that electrons had another intrinsic form of angular momentum which was named spin ($\mathbf{S}$), thus giving rise to the naming convention: $\mathbf{L}_z$ and m_l for orbital angular momentum, and $\mathbf{S}_z$ and m_s for spin angular momentum. Thus, quantum theory shows that m affects the wavefunction of an orbital state, and m takes the values $m_l = \{-l, 1-l, \ldots, 1+l, l\}$ such that $-l < m_l < l$, and similarly for m_s such that $m_s = \pm\frac{1}{2}$.

It is important to note that in the rest of this thesis, $m_l = m_{orb}$ and $m_s = m_{spin}$.

2.1.3 Principles of XAS and XMCD

X-ray absorption spectroscopy (XAS) at the $L_{2,3}$ edge involves the excitation of a 2p core electron via the absorption of an X-ray photon, causing it to transit into the 3d valence band [14]. The L_3 and L_2 transitions correspond to the excitation of a $2p_{3/2}$ and $2p_{1/2}$ electron respectively. Upon excitation of a core electron, a core hole is formed in the core shell. As XAS involves the transition of a core electron to a valence shell, the absorption spectra (measured by X-ray transmission intensity through the film) are directly affected by the valence shell properties, such as valence shell occupancy, oxidation state, and crystal structure density [14, 15].

X-ray magnetic circular dichroism (XMCD) is a variation of XAS that measures the difference in the target element's absorption of left circularly polarized light (lcp) and right circularly polarized light (rcp)[16]. The phenomenon of different absorption of left and right circularly polarized light is known as dichroism, and is defined as:

$$\Delta\mu = \mu_- - \mu_+ = \Delta\epsilon_M C\mathbf{B}\lambda \tag{2.2}$$

Where μ_- is the lcp absorption, μ_+ is the rcp absorption, $\Delta\epsilon_M$ is the differential molar absorptivity per Tesla of magnetic field, C is the molar concentration of the absorbing species, and λ is the path length through the sample[16]. Dichroism is related to the Faraday effect[16], where linearly polarized light experiences a rotation of polarization angle when travelling through a material, placed in a magnetic field, that experiences magnetically induced birefringence. It was later also understood that a magnetic field can also change a material's lcp and rcp absorptivity. Thus, XMCD utilizes this phenomena, analyzing a material's change in absorptivity. A comparison between XAS and XMCD is shown in Fig. 2.1.

In XAS, there is no differentiation between absorption of lcp or rcp x-

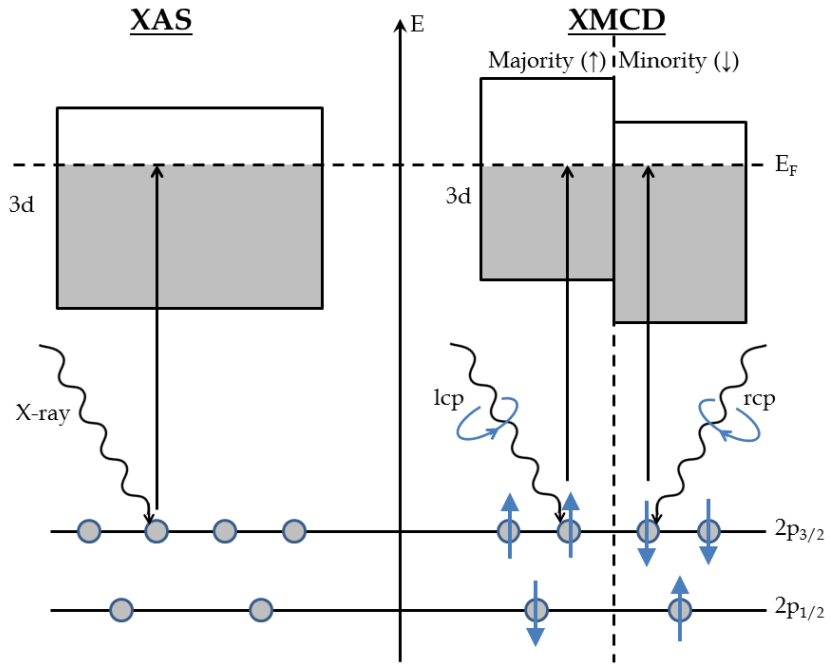

Fig. 2.1. Diagram depicting L_3 electron transition from core 2p shell to 3d valence band in XAS (left of vertical axis) and XMCD (right of vertical axis). Greyed out areas of the 3d bands are filled with electrons. E_F is the Fermi level, and the majority and minority spin are spin up and spin down respectively.

rays, so all electrons see the same density of valence states. However, in XMCD, due to the circular polarization of incoming x-rays, the electrons in the 2p shell get split into 2 sets that either transit to the majority or minority spin bands. In ferromagnetic materials like Co, Fe, and Ni, the energy bands of majority and minority spins get shifted from one another due to delocalized 3d electrons, resulting in an abundance of one spin over another[17]. Consequently, electrons in the 2p shell can only transit to either of the 2 bands, as shown in Fig. 2.1. Since spin up electrons can only absorb lcp while spin down electrons can only absorp rcp, the absorption of lcp and rcp x-rays becomes different, giving rise to dichroism.

2.1.4 X-ray Sum Rule

In non-volatile magnetic random access memory, data is stored in poly-crystalline grains. For bulk ferromagnetic materials, the spins of individual

atoms within each grain tend to align, and can be treated to have only 1 magnetic moment [18]. STT-MRAMs store data by flipping the total spin (either from up to down, or left to right or vice versa), allowing for binary data to be stored.

In 1993, Thole et. al. published the derivation of an X-ray sum rule that would allow for the determination of $\langle L_z \rangle$ and $\langle S_z \rangle$ from XMCD and XAS spectra[19, 20]:

$$\begin{aligned} \rho &= \frac{\int_{j_+ + j_-} (\mu^+ - \mu^-)\, d\omega}{\int_{j_+ + j_-} (\mu^+ + \mu^- + \mu^0)\, d\omega} \\ &= \frac{1}{2} \frac{l(l+1) + 2 - c(c+1)}{l(l+1)(4l + 2 - n)} \langle L_z \rangle \end{aligned} \tag{2.3}$$

$$\begin{aligned} \delta &= \frac{\int_{j_+} (\mu^+ - \mu^-)\, d\omega - [(c+1)/c] \int_{j_-} (\mu^+ - \mu^-)\, d\omega}{\int_{j_+ + j_-} (\mu^+ + \mu^- + \mu^0)\, d\omega} \\ &= \frac{l(l+1) - 2 - c(c+1)}{3c(4l + 2 - n)} \langle S_z \rangle \\ &+ \frac{l(l+1)[l(l+1) + 2c(c+1) + 4] - 3(c-1)^2(c+2)^2}{6lc(l+1)(4l + 2 - n)} \langle T_Z \rangle \end{aligned} \tag{2.4}$$

Where c and l are the orbital angular momentum quantum numbers for the core orbital (c=1 for Fe and Co $L_{2,3}$ edge) and valence orbital (l=2 for Fe and Co $L_{2,3}$ edge), n is the number of electrons in the valence shell (electron occupation number), ω is the energy of X-rays hitting the sample, and j_+ and j_- refer to the integration ranges of L_3 and L_2 peaks respectively. $\langle T_z \rangle$ is the expectation value of the magnetic dipole operator, which is negligible as compared to $\langle S_z \rangle$ for larger 3d transition metals (i.e. Fe, Co, Ni)[20]. From ρ and δ, one can determine the magnetic moment quantum number from the following equations[16]:

$$m_{orb} = -\langle L_z \rangle \tag{2.5}$$

$$m_{spin} = -g_s \langle S_z \rangle \tag{2.6}$$

The sum rule above was derived for bulk materials using graphical theory of angular momentum. As such, to modify the sum rule to be applicable to thin film or interface systems, an understanding of graphical theory of angular momentum is required.

Alternative form

In 1995, a paper by C. T. Chen et al. on analyzing Fe and Co thin films (5-7nm) presented a simplified, more compact form of Thole's sum rule [21]:

$$m_{orb} = -\frac{4\int_{L_3+L_2}(\mu^+ - \mu^-)\,d\omega}{3\int_{L_3+L_2}(\mu^+ + \mu^-)\,d\omega}(10 - n_{3d}) \tag{2.7}$$

,

$$\begin{aligned} m_{spin} = &-\frac{6\int_{L_3}(\mu^+ - \mu^-)\,d\omega - 4\int_{L_3+L_2}(\mu^+ - \mu^-)\,d\omega}{\int_{L_3+L_2}(\mu^+ + \mu^-)\,d\omega} \\ &\times (10 - n_{3d})\left(1 + \frac{7\langle T_z \rangle}{2\langle S_z \rangle}\right)^{-1} \end{aligned} \tag{2.8}$$

Chapter 3

Methodology

The 2 films used in this project were fabricated at the Agency for Science, Technology and Research (A*STAR) Data Storage Institute (DSI) by radio frequency (RF) magnetron sputtering with a sputtering chamber pressure was about 2×10^{-8} mbar. Fig. 3.1 shows the layer species, order, and thickness of the 2 samples. The 2 samples were grown on separate substrates.

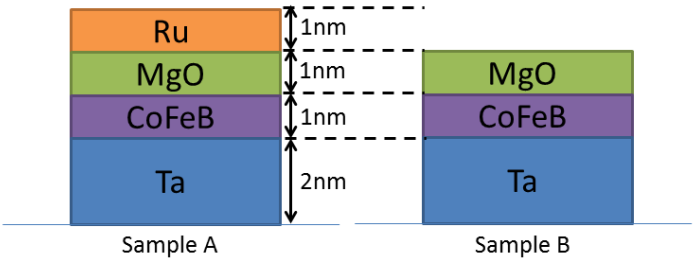

Fig. 3.1. Diagram depicting the layer order and layer thickness of the 2 samples used. Sample A has a 1nm Ru capping layer while sample B does not. Ta acts as a seed layer to the CoFeB layer.

XAS and XMCD was used to analyze the samples. In XMCD, (2.2) shows that a species' dichroism is dependent on $\Delta\epsilon_M$, an intrinsic property of a given species. This is what gives different species their characteristic XMCD spectra. Also, the dependence on molar concentration would allow one to determine the relative concentration of a species, or relative changes in molar concentration, should several species appear in the same spectra,

like that of different oxidation states [15].

As a consequence of the magnetic field, XMCD can also study otherwise energetically degenerate states due to Zeeman splitting[16]. Zeeman splitting causes electrons within the same orbital with different total angular momentum (j) to have different energy levels, thus removing degeneracy. As such, by measuring μ_- and μ_+ separately, one can find both XMCD and XAS data featuring L_3 and L_2 absorption peaks of Fe and Co separately by either taking the difference (for XMCD) or sum (for XAS) of the absorptivity for each X-ray photon energy[16].

The advantage of using XAS and XMCD is that each element has its own set of characteristic absorption edges depending on the core level involved. Thus, both methods are element specific, allowing one to study the electronic and magnetic properties of Co and Fe separately despite being in an alloy. Also, since XAS and XMCD use X-ray as a probe, it is a non-destructive method as the X-rays can penetrate through the material to measure interface effects without changing the electronic or physical structure of the film.

Synchrotron radiation was used for XAS and XMCD as other conventional X-ray sources are not able to produce X-rays of high enough intensity at the range required for XMCD[16]. (This also implies that research institutes without synchrotrons would find difficulty replicating this methodology.) As synchrotron radiation is linearly polarized in the plane of orbit[14], it should have nearly equal intensities of lcp and rcp.

The XAS and XMCD data were obtained from measurements at the Singapore Synchrotron Light Source (SSLS) SINS beamline. The measurements were done by Dr. Yu Xiaojiang (this project's co-supervisor). XAS measurements were taken at 2.3×10^{-9} mbar, with an oscillating magnetic field of ± 1 T. The photon beam was 88% linear polarized. The XMCD data was calculated from XAS, and the results for some samples

were normalized. For each sample and species, μ_+ and μ_- values with their corresponding photon energy were given to the author. After more normalization, XAS and XMCD spectra were plotted.

With the XAS and XMCD data, the X-ray sum rule was used to determine the spin and orbital magnetic moments of Fe and Co. In most works on STT-MRAM materials, only the total "magnetic moment" was discussed due to it's relation to a material's magnetization [22, 23, 24, 25]. However, as shown in Section 2.1.2, spin is a quantum theory concept, and is distinguishably different from the total and orbital magnetic moments. Consequently, it is important to be able to separately determine the orbital (m_{orb}) and spin (m_{spin}) magnetic moments of the ferromagnetic or ferrimagnetic species in materials of interest (Co and Fe in the case of the CoFeB/MgO interface).

The form of the X-ray sum rule used for data analysis was (2.7) and (2.8) instead of Thole's original equation ((2.3) and (2.4)) as this project deals with ultra thin films. Since this form of the sum rule does not account for interface effects, the magnetic moment contribution due to the interface effects alone cannot be determined directly. However, it still can show relative changes when a change is introduced to a thin film system by comparing the calculated spin and orbital magnetic moments.

Chapter 4

Results

4.1 Proof of validity of X-Ray sum rule

Before using (2.7) and (2.8) to calculate the spin and orbital magnetic moments from experimental data, it was checked whether one could reproduce the calculated magnetic moment presented by C. T. Chen[21]. DataThiefIII version 1.7 (a shareware[26]) was used to extract data points from C. T. Chen's Fe data, and the XAS and XMCD integrals of $(\mu_- + \mu_+)$ and $(\mu_- - \mu_+)$ were summed up over the required ranges to give the integrated value of the spectra. The various sums were then used to find m_{orb} and m_{spin} using (2.7) and (2.8). Comparing with C. T. Chen's calculations before correcting for $\langle T_z \rangle$, it was found that while the percentage discrepancy for m_{orb} was 22.2%, m_{spin} was very accurately reproduced with only an error of 0.9%. Since the error for m_total is still about 0.9%, which shows that the author's calculations were still sufficiently good to use on experimental data. In Chapter 7, the importance of eradicating this error in application of the sum rule is elaborated on.

4.2 XAS and XMCD Results

Fig. 4.1 and Fig. 4.2 show the XAS and XMCD data obtained for both samples for the Fe and Co $L_{2,3}$ edge respectively. All data obtained was normalized to make comparisons between spectral features easier. Due to the difference in film thickness between samples, one cannot simply compare absorption intensity between samples. However, the relative peak heights (or peak heights relative to the background step increment) for each sample can be used to reflect changes in occupation ratios of different species that contribute to different spectroscopic features. This section will highlight the features of the XAS and XMCD spectra.

For Fig. 4.1, data was normalized to give nearly the same amount of background absorption. For the sample without a capping layer, the XMCD and XAS peaks align, and are similar to that of thin Fe films [21]. However, upon addition of the capping layer, peak splitting/ forming of a new peak was observed in the L_3 XAS peak, and a higher energy shoulder can be seen for the L_2 peak. Also, the XAS peaks of the sample with capping did not align with the XMCD peaks.

For Fig. 4.2, an amazing observation can be made: the addition of a capping layer caused the inversion of the XMCD. The XAS plots reveal that although there is a small shift in peak position, the form of the spectrum with or without capping is roughly the same. The lack of background step increment in absorption for the sample with capping was due to the Co signal being initially relatively weak as compared to iron. Consequently, the addition of an extra capping layer resulted in the drowning out of the step background (the film was 6nm thick, while the penetration depth of X-rays are $\leq\sim$ 10nm[15]). Once again, like for the Fe XAS and XMCD, the peak positions align when there is no capping layer, and do not align when there is a capping layer.

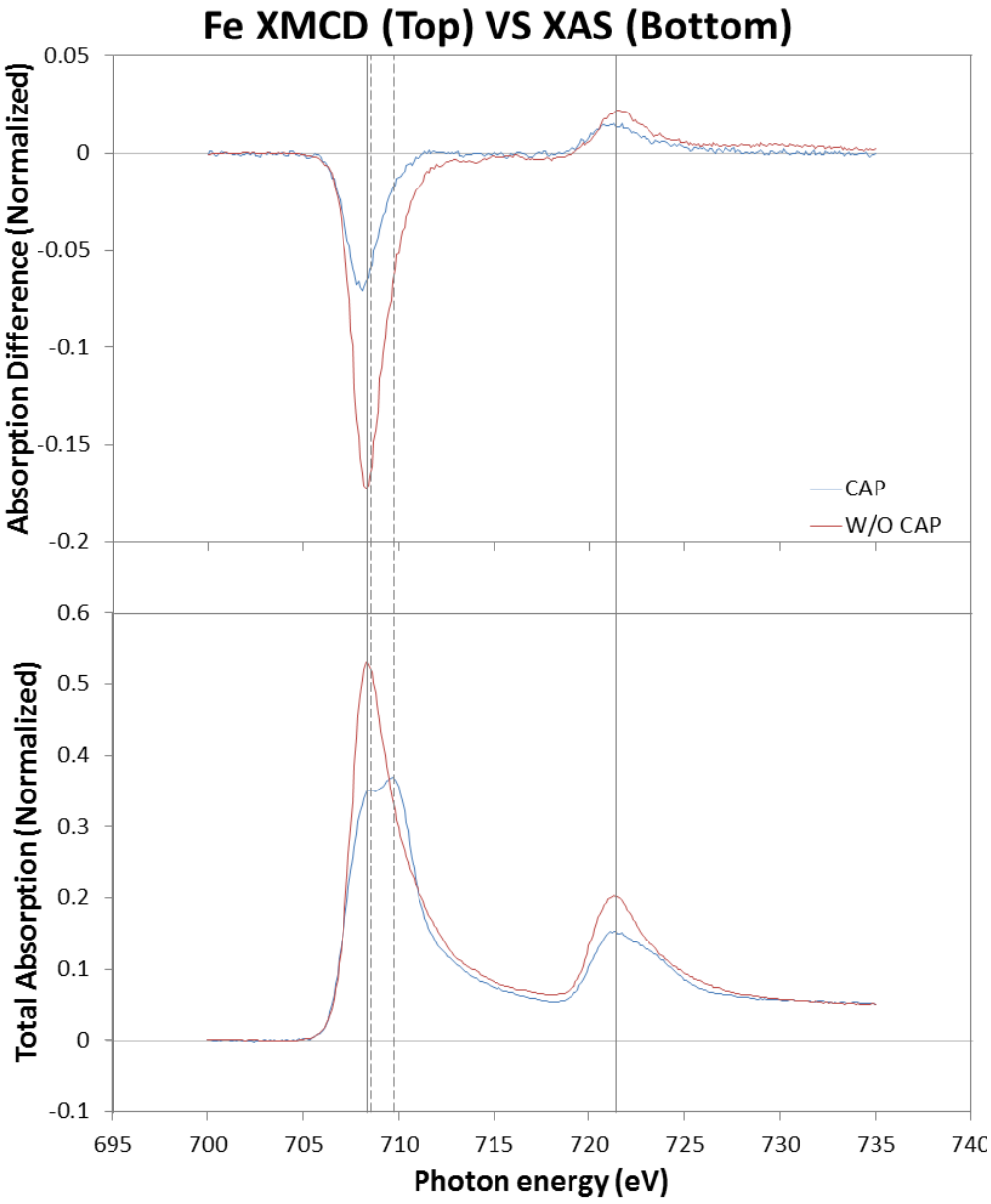

Fig. 4.1. XMCD (top) and XAS (bottom) of the 2 samples taken at the Fe $L_{2,3}$ range. Solid lines refer to XAS peaks from the sample without capping while the dotted lines mark the XAS peaks of the sample with capping. At 723 eV, the peaks for both with and without capping align.

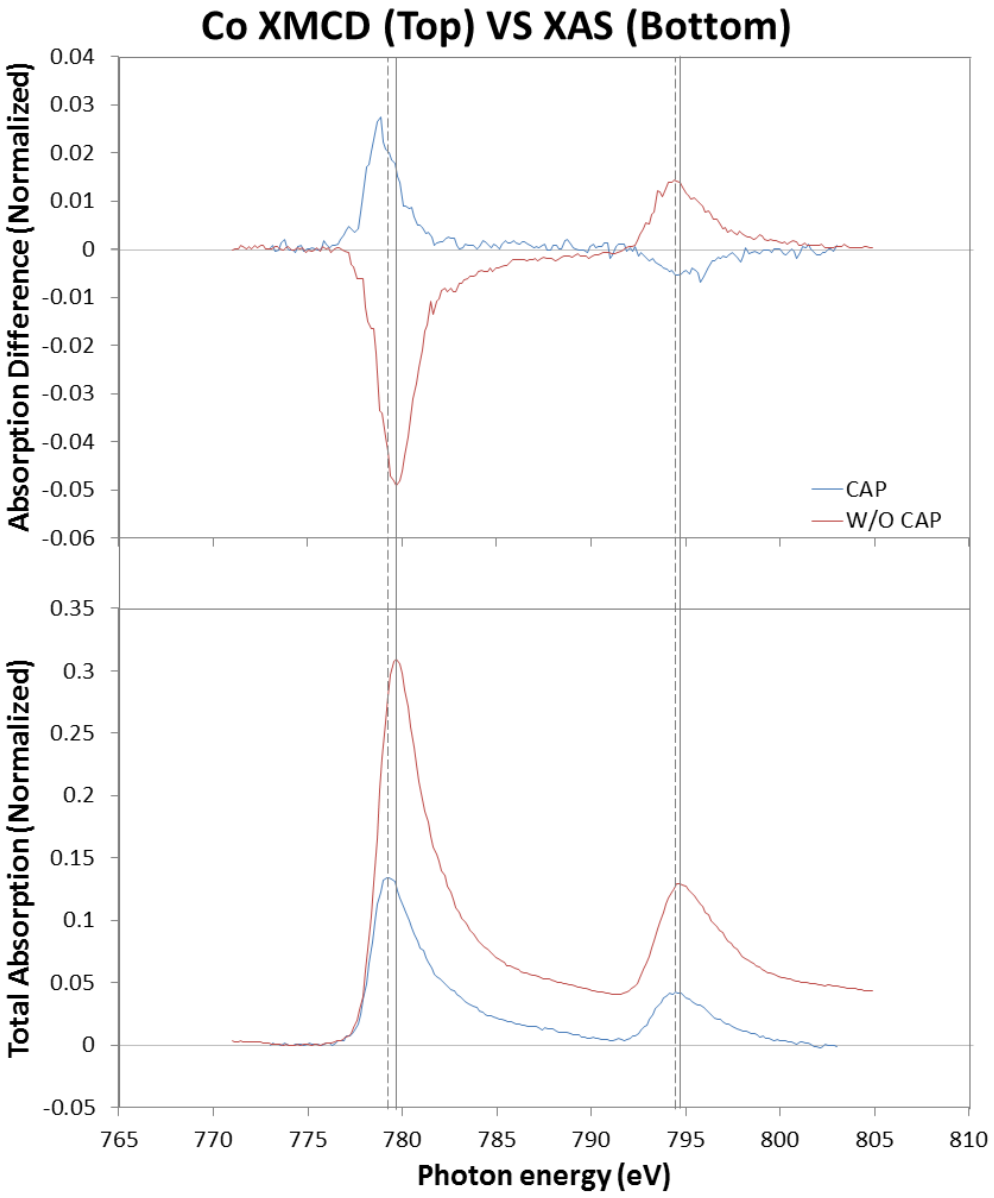

Fig. 4.2. XMCD (top) and XAS (bottom) of the 2 samples taken at the Co $L_{2,3}$ range. Solid lines refer to XAS peaks from the sample without capping while the dotted lines mark the XAS peaks of the sample with capping.

4.3 Magnetic moment of Co and Fe

The application of the X-ray sum rule required the integration of the XMCD and XAS spectra. For XAS, there exists an L_3 and L_2 step jump due to transitions (corresponding to absorption) that are not sensitive to the polarization of light (μ_0). The height of the step is dependent on the relative degeneracy of the $2p_{3/2}$ and $2p_{1/2}$ orbitals (2:1)[27] and this step background had to be subtracted from the integral as they are absorptions that do not reflect the dichroism of the material. Fig. 4.3 shows the step functions used. The form of the step function was taken from other literature[21], and scaled for each of the XAS spectra.

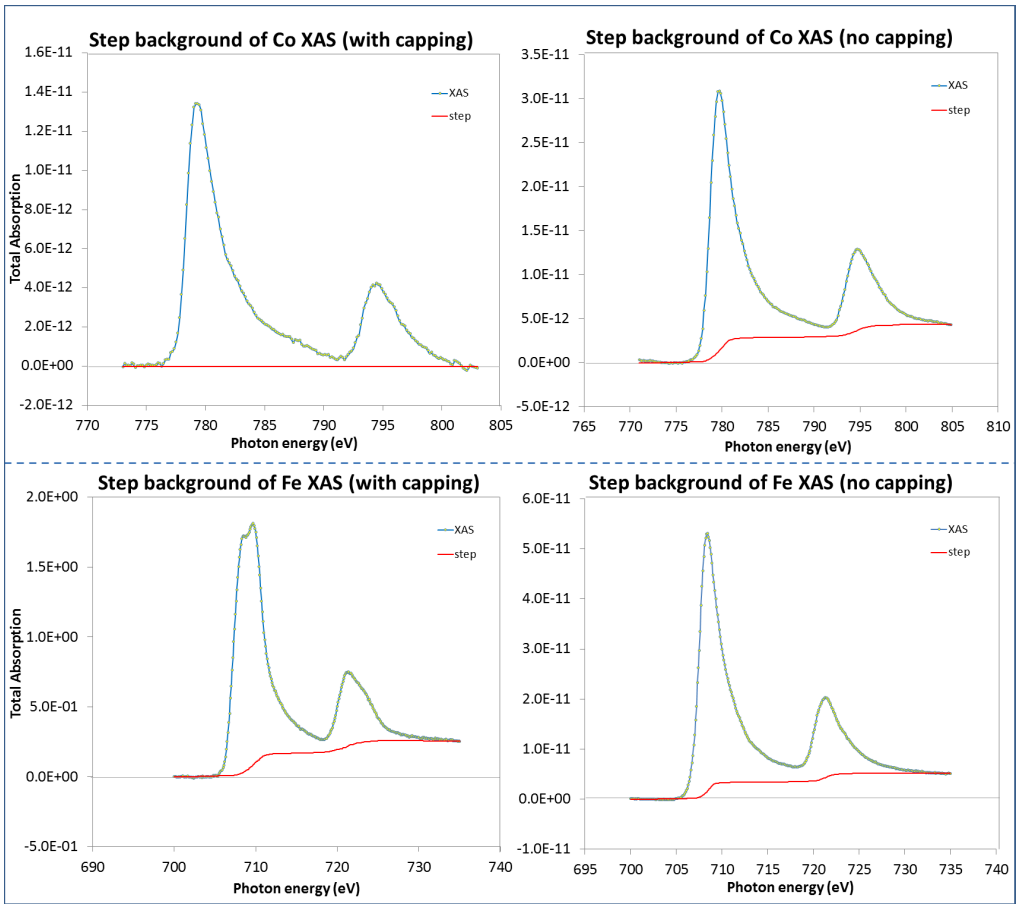

Fig. 4.3. Graphs of the 4 XAS plots determined from experimental data, plot against the two-step function used to subtract the L_3 and L_2 step jump background from the XAS integral, $\int_{L_3+L_2}(\mu^+ + \mu^-)\,d\omega$. For the Co XAS of the sample with capping, the initially weak signal from Co, compounded with scattering through the extra 1nm Ru layer, resulted in the background getting drowned out.

The calculated magnetic moments were compared as shown in Table 4.1. Magnetic moments of the sample with capping were noticeably lower than that of the sample without capping. Also, the m_{orb}/m_{spin} decreased with capping for Fe, and increased for Co. Most importantly, Co experienced a change of sign for both orbital and spin magnetic moments.

Table 4.1
Table of magnetic moments calculated from experimental data in units of μ_B per atom, where μ_B is the Bohr's magneton. n_{3d} for Fe and Co were taken to be 6.61 and 7.51 respectively [21].

Sample	Fe m_{orb}	Fe m_{spin}	Fe m_{orb}/m_{spin}
No capping	0.528	1.60	0.329
With capping	0.213	0.845	0.252
Sample	Co m_{orb}	Co m_{spin}	Co m_{orb}/m_{spin}
No capping	0.198	0.817	0.242
With capping	-0.204	-0.430	0.475

Chapter 5

Discussion

The most surprising observation from the data was the flip of the XMCD spectra of Co when there was a capping layer. The next surprising observation was the formation of higher energy peak and the high energy shoulder, in the L_3 and L_2 XAS peaks of Fe respectively, but not in its XMCD spectra. Other studies on Co and Fe using both XAS and XMCD reveal that it is normal for slight misalignments of XAS and XMCD peaks[28, 29, 30]. As such, peak alignment would not be discussed in this section.

The Fe and Co spectral shape for the sample without capping most closely resembles that of metallic Fe and Co (comparing peak postition and alignment with other literature [15, 31]). Upon introduction of a capping layer, XAS reveals that Fe seems to exhibit extramultiplet features. Since there was no change in the spectral shape of the XMCD, and considering the relative position of the new peak, the new peak is highly similar to what could have been due to antiferromagnetic Fe^{2+}[29]. However, as shown by the analysis by A*STAR DSI, the change in Fe XAS spectra was not due to the introduction of oxygen into the CoFeB layer. If there was oxygen in the alloy layer, it would have very likely created other ionization states in Co as well[15]. However, since the position of the Fe^{2+} peak is dependent on the structure, and is usually found on the lower energy side of the metallic

Fe peak [32, 15], it remains unclear whether the new peak corresponds to Fe^{2+}.

No matter the oxidation state of the new peak, it still represents the existance of another state of Fe besides metallic Fe. It is thus proposed that the new electronic state reflected in the Fe XAS was due to charge transfer from the Ru capping layer, which donated electrons to the Fe atoms at the interface, giving it ferrimagnetic properties. This is possible as Ru has a large electron cloud that can be easily distorted to donate electrons, or possibly interact with the electron clouds of other atoms [33]. This explanation makes it more probable that the new peak was due to the existence of Fe^{2+}.

Another interesting conclusion can be drawn from the XAS data: Since the signal from the new electronic state in Fe was stronger than that of metallic Fe, it might imply that only the Fe atoms closer to the surface of the film ($\sim$ 2nm deep) were affected by the capping layer. This is because the signal strength weakens as the photon beam penetrates the material, resulting in a larger response from the interface (with affected Fe atoms) than the metallic Fe atoms deeper in the thin film.

The possibility of a capping layer affecting interface atoms could be used to explain the flip of XMCD in Co. As can be seen from the XAS, it seems that in both samples, the XAS was similar to that of metallic Co, except that the step background was reduced in the sample with capping. The change of peak sign resulted in the calculated magnetic moments being negative. Thus, there are 2 questions to be answered: What could have caused the change in response to the polarization of light absorbed (dichroism), and what is the significance of a negative magnetic moment? In metallic Co and Fe, negative XMCD peaks reflect an abundance of the majority spin (spin up) and the positive peaks reflect an abundance of minority spin (spin down). As can be seen in the Co XMCD for the sample

with capping, it is like as if the band of the majority and minority states had shifted relative to each other such that the majority spin states were more filled than the minority spin states. This suggests that spin-orbit coupling between the Fe and Co orbitals at the CoFeB/MgO interface induced a change in the Co spin majority and minority bands due to the change in Fe electronic orbitals by charge transfer from the capping layer. This also hints that the role of oxygen at the interface might be to induce Fe 3d hybridization with O 2p, which then coupled with Co to produce magnetic anisotropy at the CoFeB/MgO interface.

Looking at Table 4.1, (2.7) and (2.8) reveal that a decrease in m_{orb} after the addition of capping was either due to the total integrated XMCD being relatively less negative than the integrated XAS, or due to a decrease in electron occupancy of the 3d orbital. For m_{spin}, either the integral of 2 L_3 XMCD peaks and 4 L_2 XMCD peaks became relatively less negative, or the occupancy decreased as well. A change in occupancy was unlikely to be the only cause because the factor that the magnetic moments that each element decreased by was not the same (Refer to Appendix A). This means that there most probably was a reduction in the L_3 XMCD peak height relative to the L_2 XMCD peak as well. Since there was other evidence of the capping layer's interaction with the interface, it was possible that the large electron cloud of Ru was able to induce hybridization effects at the interface for both Fe and Co[34]. Hybridization causes the broadening of Fe and Co bands, resulting in a larger overlap of spin up and spin down states, and thus a reduction of the difference between XMCD peak intensities of L_3 and L_2[34]. However, the significance of a negative magnetic moment still needs to be answered.

Interpretation of the experimentally determined magnetic moments by quantum theory gives insight into the significance of negative magnetic moments: As mentioned in Section 2.1.2, m_{orb} and m_{spin} are directional

quantum numbers of angular momentum. For a single particle (quantum), it was derived that m should have a value that should be either integer or half-integer depending on the value of l and s. However, the values determined experimentally revealed that it was not the case. This suggests 2 things: Interactions between neighbouring atoms in an extended solid state material resulted in a change in the extent of magnetization in the direction of the external magnetic field (z-direction); and there was an alteration of the orbital wavefunctions which were involved in the magnetic properties of the material. Comparing with literature[21], the percentage differences between the magnitudes of the magnetic moments of Fe and Co for the sample without capping with reported Fe and Co magnetic moments from Fe thin films and Co thin films were large ($> 21\%$). This supports other literature[35], that the hybridization of the Fe 3d and O 2p orbitals (showing interactions with other atoms) at the CoFeB/MgO interface gives rise to PMA at the interface. However, whether this is the only effect of oxygen at the interface remains unclear, and left for further studies (See Chapter 7).

After the addition of a capping layer (not in contact with the interface) the magnetic moment experienced another change. This implies that the addition of a capping layer managed to affect the orbital wavefunction of the atoms at the interface, thus agreeing with the XMCD and XAS data – the atoms at the capping layer had possibly interacted with the interface atoms via charge transfer across the MgO layer. Focusing on the negative m_{orb} and m_{spin} observed, it implies that the spin orientation relative to the external magnetic field direction has "flipped"(such that the $\mathbf{m}_{orb}$ and $\mathbf{m}_{spin}$ vectors now point in the opposite direction of the $\mathbf{L}_z$ and $\mathbf{S}_z$ vectors respectively). This is an interesting new phenomenon, and deeper research into the effects of capping could reveal new physics which can shed light on how capping can be manipulated for optimization of data storage technology. In this

experiment, however, this poses a problem for practical applications as Co, with capping, would reduce the total magnetic moment, of the interface as Fe still has positive magnetic moment.

Sources of error in this experiment and how to reduce them are addressed in Chapter 7.

Chapter 6

Conclusion

In conclusion, it was found that the addition of a 1nm Ru capping layer on top of a CoFeB/MgO interface resulted in multiplet effects in Fe, and an unexpected flip of spin magnetic moment only in Co. The magnetic moments of Fe and Co atoms were also determined, where Co experienced a change in sign of both spin and orbital magnetic moments. It was thus proposed that this was due to charge transfer from the capping layer to Fe, followed by spin-orbit coupling between Fe and Co electrons. Also, as oxygen was not found in CoFeB, it was concluded that the role of oxygen was most likely to induce Fe 3d and O 2p hybridization, which affected the orbitals of Co via spin-orbit coupling and induced magnetic anisotropy at the CoFeB/MgO interface.

Chapter 7

Future work

Throughout the course of this project, the author had many ideas of what could be done to improve on this project, but could not due to time constraints. This section will highlight the different areas that the author felt should be done to reach certain targets not reached in this project. The 4 research questions in this project were as follows:

1. What are the spin and orbital magnetic moments of Co and Fe atoms at a CoFeB/MgO interface?

2. How can interface characteristics be isolated from XAS and XMCD data and differentiated from known bulk characteristics? (i.e. How to identify magnetic anisotropy?)

3. How can the effects of the capping layer be isolated?

4. How can the effects of oxygen (carrier) be isolated from the rest of the data and be interpreted?

The pursuit of more accurate answers to these questions remain meaningful for future works as assumptions were made in the execution of this project:

As mentioned in Section 2.1.4, the derivation of the X-ray sum rule by Thole ((2.3) and (2.4)) requires the understanding of the graphical theory

of angular momentum. After a month of learning the graphical theory, the author realized that the X-ray sum rule requires an in-depth understanding of the graphical method to understand the physical significance behind each step of the derivation. Understanding the derivation would allow one to know the physical assumptions and constraints considered in the derivation. For example, a work by Altarelli[36] showed a simple, alternative proof for Thole's sum rule and mentioned the assumptions used in Thole's derivation. If one understands the physics behind thin films and interfaces, one can apply new constraints to modify the bulk form to fit that for interface conditions. Such a new form would be useful for future research on interface materials, and would only be possible if one has a deeper understanding of the graphical theory of angular momentum.

Concerning the correct usage of the X-ray sum rule, C. T. Chen's form of the sum rule was used even though the discrepancy for m_{orb} was high. Also, the experimental m_{orb}/m_{spin} was nearly 10 times larger than that found in the replication of literature values, indicating that the calculation discrepancy error (22.2%) from m_{orb} was no longer negligible. If this form of the sum rule were to be used in future work, the cause for the high discrepancy should be identified and reduced for more accurate use of the sum rule, and determination of m_{orb}. Alternatively, data analysis softwares like IGOR Pro by WaveMetrics can be used for more accurate determination of the magnetic moments. IGOR was not used in this project due to time constraints, as the use of the software required time to learn. Besides, blind usage of the software without understanding the physics behind Thole's X-ray sum rules, (2.7) and (2.8) would not allow the researcher to appreciate the changes in calculated magnetic moment (like changes due to a reduction in intensity difference in the L_2 and L_3 in XMCD). Before use of IGOR, it should also be checked whether IGOR can reproduce the calculated magnetic moment from known literature.

In the use of the sum rule, the value of Co and Fe n_{3d} were taken to be 7.51 and 6.61 respectively. These values were taken from C. T. Chen's work and assumed to be close to that in this project's samples [21]. Also, n_{3d} was taken to be unchanging during the calculation of the magnetic moments. The values listed above were calculated by integrating the density of states using band theory[37, 38], as atoms in bulk have different electron occupation than the atomic state (7 and 6 electrons for Co and Fe respectively). However, at an interface, conventional band theory would not apply anymore as interface effects can affect the occupation and density states, as shown in this project. Thus, for more accurate determination of the magnetic moments, n_{3d} should be measured for both elements for both samples. n_{3d} can be determined for alloys xia X-ray photoemission spectroscopy (XPS) and inverse XPS[39], or relative changes in n_{3d} between samples can be determined using electron energy loss spectroscopy (EELS)[40]. Studies on the density of states of Co and Fe at the CoFeB/MgO interface could be a whole research project on its own as it has been shown that the concentration ratio of Co to Fe in the film would affect the density of states, and thus the XMCD and calculated magnetic moments [29]. Understanding how the density of states varies with concentration might shed light on how to maximize the density of states for Co and Fe to manipulate the spin and orbital magnetic moments of Co and Fe.

On the research questions concerning isolation of characteristics, one should first have a better understanding of solid state physics. Areas that the author had identified (but was unable to get a sufficient understanding of due to time constraints), were crystal field theory and charge transfer dynamics. An understanding of crystal field theory would allow one to better understand bulk material behaviour, or simply how atoms in an extended solid interact with each other to produce properties not seen in individual atoms or molecules. More importantly, a better understanding

of charge transfer would allow one to evaluate whether the hypothesis suggested in this project (that the Ru capping layer affects the interface via charge transfer) is possibly correct. It would also allow one to have a better understanding of how oxygen could possibly act as a charge carrier at the interface, and how it would affect the interface atoms to show changes in the XMCD and XAS.

Also, data from more samples could be obtained. In this project, the author was only provided with 2 samples as she was told that they were representative of other similar samples. However, for thorough scientific research, one should have more samples to ensure consistency of observations. Also, it would allow one to determine the uncertainty of experimental magnetic moments to evaluate the accuracy of measurement of the method used in this project (Refer to Chapter 3. Also, by having more types of samples (e.g. samples with thinner/ thicker MgO, Ta or Ru capping layer, or different layer order, or different capping material such as Ta) it might give better insight into the viability of charge transfer being the cause of the phenomena, or drive attention to other possible factors that might have led to the flip in magnetic moment: What if the interface Co was affected by the Ru/MgO interface, and not just Ru? To what extent can spin-orbit coupling between the Fe^2 state and Co affect the spin of Co electrons (i.e. how significant is the contribution by spin-orbit coupling)? It has been shown that the presence of Fe^{2+} alone does not cause the flipping of magnetic moment[29], so it is likely that some new phenomenon related to charge transfer from the capping layer caused the inversion of Co XMCD. However, why were multiplet effects not observed in Co, and the flip in spin not observed in Fe? These are important questions to be answered, and require a lot more time for literature research and understanding of first-principles.

Lastly, even if all the above points addressed, there were little studies

done on the morphology of the film (the author was only told that no oxygen was found in the CoFeB layer). Since the proposed hypothesis concerned charge transfer, the direction of future work should be focused on increasing the MgO layer thickness, and reducing the Ru, CoFeB, and Ta layer thickness to still allow the film to be adequately analyzed by XAS and XMCD (since the Co intensity was weak in the first place, the total film thickness should be kept as thin as possible). Thinner layers can be made by using molecular beam epitaxy (MBE). The thicker the MgO layer, the less Ru should be able to affect the interface. Alternatively, Mg can be substituted for more electronegative metals (like aluminium). Due to the higher electronegativity than Mg, it should have a higher tendency to retain the Ru electron cloud within the oxide layer. Thus, it would be expected that the multiplet effect in Fe would be reduced, and so would the inversion of Co XMCD. However, the increased electronegativity would also affect the hybridization of Fe 3d and O 2p orbitals, so this has to be taken into consideration during analysis as well.

Bibliography

[1] S. Iihama, S. Mizukami, H. Naganuma, M. Oogane, Y. Ando, and T. Miyazaki, "Gilbert damping constants of ta/cofeb/mgo(ta) thin films measured by optical detection of precessional magnetization dynamics," *Phys. Rev. B*, vol. 89, p. 174416, May 2014. [Online]. Available: http://link.aps.org/doi/10.1103/PhysRevB.89.174416

[2] S. Ikeda, J. Hayakawa, Y. Ashizawa, Y. M. Lee, K. Miura, H. Hasegawa, M. Tsunoda, F. Matsukura, and H. Ohno, "Tunnel magnetoresistance of 604300k by suppression of ta diffusion in cofebmgocofeb pseudo-spin-valves annealed at high temperature," *Applied Physics Letters*, vol. 93, no. 8, 2008. [Online]. Available: http://scitation.aip.org/content/aip/journal/apl/93/8/10.1063/1.2976435

[3] H. D. Gan, H. Sato, M. Yamanouchi, S. Ikeda, K. Miura, R. Koizumi, F. Matsukura, and H. Ohno, "Origin of the collapse of tunnel magnetoresistance at high annealing temperature in cofeb/mgo perpendicular magnetic tunnel junctions," *Applied Physics Letters*, vol. 99, no. 25, 2011. [Online]. Available: http://scitation.aip.org/content/aip/journal/apl/99/25/10.1063/1.3671669

[4] S. Ikeda, K. Miura, H. Yamamoto, K. Mizunuma, H. D. Gan, M. Endo, S. Kanai, J. Hayakawa, F. Matsukura, and H. Ohno, "A perpendicular-anisotropy cofebmgo magnetic tunnel junction,"

Nature Materials, vol. 9, no. 9, p. 721, 2010. [Online]. Available: http://www.nature.com/nmat/journal/v9/n9/full/nmat2804.html

[5] V. W. Guo, B. Lu, X. Wu, G. Ju, B. Valcu, and D. Weller, "A survey of anisotropy measurement techniques and study of thickness effect on interfacial and volume anisotropies in copt multilayer media," *Journal of Applied Physics*, vol. 99, no. 8, 2006. [Online]. Available: http://scitation.aip.org/content/aip/journal/jap/99/8/10.1063/1.2169540

[6] M. Johnson, R. Jungblut, P. Kelly, and F. den Broeder, "Perpendicular magnetic anisotropy of multilayers: recent insights," *Journal of Magnetism and Magnetic Materials*, vol. 148, no. 12, pp. 118 – 124, 1995. [Online]. Available: http://www.sciencedirect.com/science/article/pii/0304885395001743

[7] Y. A. Bychkov and E. I. Rashba, "Oscillatory effects and the magnetic susceptibility of carriers in inversion layers," *Journal of Physics C: Solid State Physics*, vol. 17, no. 33, p. 6039, 1984. [Online]. Available: http://stacks.iop.org/0022-3719/17/i=33/a=015

[8] A. Matos-Abiague and J. Fabian, "Anisotropic tunneling magnetoresistance and tunneling anisotropic magnetoresistance: Spin-orbit coupling in magnetic tunnel junctions," *Phys. Rev. B*, vol. 79, p. 155303, Apr 2009. [Online]. Available: http://link.aps.org/doi/10.1103/PhysRevB.79.155303

[9] I. Žutić, J. Fabian, and S. Das Sarma, "Spintronics: Fundamentals and applications," *Rev. Mod. Phys.*, vol. 76, pp. 323–410, Apr 2004. [Online]. Available: http://link.aps.org/doi/10.1103/RevModPhys.76.323

[10] H. X. Yang, M. Chshiev, B. Dieny, J. H. Lee, A. Manchon, and K. H. Shin, "First-principles investigation of the very large

perpendicular magnetic anisotropy at fe|mgo and co|mgo interfaces," *Phys. Rev. B*, vol. 84, p. 054401, Aug 2011. [Online]. Available: http://link.aps.org/doi/10.1103/PhysRevB.84.054401

[11] H. Lth, *Solid Surfaces, Interfaces and Thin Films*, 6th ed., ser. Graduate Texts in Physics. Springer International Publishing, 2015.

[12] R. A. F. H. D. Young, *Sears and Zemansky's University Physics*, 11th ed. San Francisco, California: Pearson/Addison Wesley, 2004.

[13] R. L. Brooks, *The Fundamentals of Atomic and Molecular Physics*, ser. Undergraduate Lecture Notes in Physics. Springer New York, 2013.

[14] B. K. Agarwal, *X-Ray Spectroscopy*, 2nd ed., ser. Springer Series in Optical Sciences. Springer International Publishing, 1991, vol. 15.

[15] D. H. Kim, H. J. Lee, G. Kim, Y. S. Koo, J. H. Jung, H. J. Shin, J.-Y. Kim, and J.-S. Kang, "Interface electronic structures of batio$_3$@x nanoparticles ($x = \gamma$-fe$_2$o$_3$, fe$_3$o$_4$, α-fe$_2$o$_3$, and fe) investigated by xas and xmcd," *Phys. Rev. B*, vol. 79, p. 033402, Jan 2009. [Online]. Available: http://link.aps.org/doi/10.1103/PhysRevB.79.033402

[16] W. R. Mason, *A Practical Guide to Magnetic Circular Dichroism Spectroscopy*, 1st ed. John Wiley and Sons, Inc., 2007.

[17] A. Scherz, *Spin Dependent X-ray Absorption Spectroscopy of 3d Transition Metals: Systematics and Applications*. dissertation.de, 2004.

[18] C. Tannous and J. Gieraltowski, "The stonerwohlfarth model of ferromagnetism," *European Journal of Physics*, vol. 29, no. 3, p. 475, 2008. [Online]. Available: http://stacks.iop.org/0143-0807/29/i=3/a=008

[19] B. T. Thole, P. Carra, F. Sette, and G. van der Laan, "X-ray circular dichroism as a probe of orbital magnetization," *Phys. Rev. Lett.*, vol. 68, pp. 1943–1946, Mar 1992. [Online]. Available: http://link.aps.org/doi/10.1103/PhysRevLett.68.1943

[20] P. Carra, B. T. Thole, M. Altarelli, and X. Wang, "X-ray circular dichroism and local magnetic fields," *Phys. Rev. Lett.*, vol. 70, pp. 694–697, Feb 1993. [Online]. Available: http://link.aps.org/doi/10.1103/PhysRevLett.70.694

[21] C. T. Chen, Y. U. Idzerda, H.-J. Lin, N. V. Smith, G. Meigs, E. Chaban, G. H. Ho, E. Pellegrin, and F. Sette, "Experimental confirmation of the x-ray magnetic circular dichroism sum rules for iron and cobalt," *Phys. Rev. Lett.*, vol. 75, pp. 152–155, Jul 1995. [Online]. Available: http://link.aps.org/doi/10.1103/PhysRevLett.75.152

[22] J. C. Sankey, Y.-T. Cui, J. Z. Sun, J. C. Slonczewski, R. A. Buhrman, and D. C. Ralph, "Measurement of the spin-transfer-torque vector in magnetic tunnel junctions," *Nature Physics*, vol. 4, no. 1, pp. 67–71, 01 2008, copyright - Copyright Nature Publishing Group Jan 2008; Last updated - 2012-11-20. [Online]. Available: http://libproxy1.nus.edu.sg/login?url=http://search.proquest.com/docview/194652316?accountid=13876

[23] D. Apalkov, A. Khvalkovskiy, S. Watts, V. Nikitin, X. Tang, D. Lottis, K. Moon, X. Luo, E. Chen, A. Ong, A. Driskill-Smith, and M. Krounbi, "Spin-transfer torque magnetic random access memory (stt-mram)," *J. Emerg. Technol. Comput. Syst.*, vol. 9, no. 2, pp. 13:1–13:35, May 2013. [Online]. Available: http://doi.acm.org.libproxy1.nus.edu.sg/10.1145/2463585.2463589

[24] J. Sun and D. Ralph, "Magnetoresistance and spin-transfer torque in magnetic tunnel junctions," *Journal of Magnetism and Magnetic Materials*, vol. 320, no. 7, pp. 1227 – 1237, 2008. [Online]. Available: http://www.sciencedirect.com/science/article/pii/S0304885307010177

[25] V. Alijani, J. Winterlik, G. H. Fecher, and C. Felser, "Tuning the magnetism of the heusler alloys mn3xcoxga from soft and half-metallic to hard-magnetic for spin-transfer torque applications," *Applied Physics Letters*, vol. 99, no. 22, 2011. [Online]. Available: http://scitation.aip.org/content/aip/journal/apl/99/22/10.1063/1.3665260

[26] B. Tummers, "DataThief III a shareware for extracting data points from graph images," http://datathief.org/, 2006.

[27] D. K. S. K. L. D'Amico, L. J. Terminello, Ed., *Synchrotron Radiation Techniques in Industrial, Chemical, and Materials Science*. Springer US, 1996.

[28] M. J. Duignan, J. P. Cunniffe, P.-A. Glans, E. Arenholz, C. McGuinness, and J. F. McGilp, "Temperature dependent studies of capped magnetic nanowires using xmcd," *physica status solidi (b)*, vol. 253, no. 2, pp. 241–246, 2016. [Online]. Available: http://dx.doi.org/10.1002/pssb.201552488

[29] S. Gautam, S. N. Kane, B. Park, J. Kim, L. Varga, J. Song, and K. H. Chae, "{XAS} and {XMCD} studies of amorphous feco-based ribbons," *Journal of Non-Crystalline Solids*, vol. 357, no. 1113, pp. 2228 – 2231, 2011, 17th International Symposium on Non-Oxide and New Optical Glasses (XVII ISNOG). [Online]. Available: http://www.sciencedirect.com/science/article/pii/S0022309310009531

[30] M. Sicot, S. Andrieu, F. Bertran, and F. Fortuna, "Probing interfacial properties of ferromagnetic/insulator bilayers with x-ray spectroscopies: Application to fe, co, mn/mgo(0 0 1) interfaces," *Materials Science and Engineering: B*, vol. 126, no. 23, pp. 151 – 154, 2006, {EMRS} 2005, Symposium B, Spintronics. [Online]. Available: http://www.sciencedirect.com/science/article/pii/S0921510705006124

[31] A. Baruth, D. J. Keavney, J. D. Burton, K. Janicka, E. Y. Tsymbal, L. Yuan, S. H. Liou, and S. Adenwalla, "Origin of the interlayer exchange coupling in [CoPt]NiO[CoPt] multilayers studied with xas, xmcd, and micromagnetic modeling," *Phys. Rev. B*, vol. 74, p. 054419, Aug 2006. [Online]. Available: http://link.aps.org/doi/10.1103/PhysRevB.74.054419

[32] T. S. Herng, W. Xiao, S. M. Poh, F. He, R. Sutarto, X. Zhu, R. Li, X. Yin, C. Diao, Y. Yang, X. Huang, X. Yu, Y. P. Feng, A. Rusydi, and J. Ding, "Achieving a high magnetization in sub-nanostructured magnetite films by spin-flipping of tetrahedral fe3+ cations," *Nano Research*, vol. 8, no. 9, pp. 2935–2945, 2015. [Online]. Available: http://dx.doi.org/10.1007/s12274-015-0798-7

[33] Y. Liu, J. Zhang, S. Wang, S. Jiang, Q. Liu, X. Li, Z. Wu, and G. Yu, "Ru catalyst-induced perpendicular magnetic anisotropy in mgo/cofeb/ta/mgo multilayered films," *ACS Applied Materials & Interfaces*, vol. 7, no. 48, pp. 26 643–26 648, 2015, pMID: 26565747. [Online]. Available: http://dx.doi.org/10.1021/acsami.5b08385

[34] F. Wilhelm, U. Bovensiepen, A. Scherz, P. Poulopoulos, A. Ney, H. Wende, G. Ceballos, and K. Baberschke, "Manipulation of the curie temperature and the magnetic moments of ultrathin ni and co films by cu-capping," *Journal of Magnetism and Magnetic Materials*,

vol. 222, no. 12, pp. 163 – 167, 2000. [Online]. Available: http://www.sciencedirect.com/science/article/pii/S030488530000531X

[35] R. Shimabukuro, K. Nakamura, T. Akiyama, and T. Ito, "Electric field effects on magnetocrystalline anisotropy in ferromagnetic fe monolayers," *Physica E: Low-dimensional Systems and Nanostructures*, vol. 42, no. 4, pp. 1014 – 1017, 2010, 18th International Conference on Electron Properties of Two-Dimensional Systems. [Online]. Available: http://www.sciencedirect.com/science/article/pii/S1386947709005463

[36] M. Altarelli, "Orbital-magnetization sum rule for x-ray circular dichroism: A simple proof," *Phys. Rev. B*, vol. 47, pp. 597–598, Jan 1993. [Online]. Available: http://link.aps.org/doi/10.1103/PhysRevB.47.597

[37] R. Wu and A. J. Freeman, "Limitation of the magnetic-circular-dichroism spin sum rule for transition metals and importance of the magnetic dipole term," *Phys. Rev. Lett.*, vol. 73, pp. 1994–1997, Oct 1994. [Online]. Available: http://link.aps.org/doi/10.1103/PhysRevLett.73.1994

[38] G. Y. Guo, H. Ebert, W. M. Temmerman, and P. J. Durham, "First-principles calculation of magnetic x-ray dichroism in fe and co multilayers," *Phys. Rev. B*, vol. 50, pp. 3861–3868, Aug 1994. [Online]. Available: http://link.aps.org/doi/10.1103/PhysRevB.50.3861

[39] G. Connell, S.-J. Oh, J. Allen, and R. Allen, "The electronic density of states of amorphous yfe and tbfe alloys," *Journal of Non-Crystalline Solids*, vol. 6162, Part 2, pp. 1061 – 1066, 1984, proceedings of the Fifth International Conference on Liquid and Amorphous Metals. [Online]. Available: http://www.sciencedirect.com/science/article/pii/0022309384906811

[40] D. H. Pearson, C. C. Ahn, and B. Fultz, "White lines and d -electron occupancies for the 3 d and 4 d transition metals," *Phys. Rev. B*, vol. 47, pp. 8471–8478, Apr 1993. [Online]. Available: http://link.aps.org/doi/10.1103/PhysRevB.47.8471

Appendix A

Percentage discrepancy calculations

Table A.1
Table of the ratios of m_{orb} and m_{spin} for the sample without capping over the sample with capping for Co and Fe. If the decrease in magnetic moment was due only to n_{3d}, $m_{orb,nocap}/m_{orb,cap}$ should equal to $m_{spin,nocap}/m_{spin,cap}$ for each element.

Species	$m_{orb,nocap}/m_{orb,cap}$	$m_{spin,nocap}/m_{spin,cap}$
Co	-1.03	-0.53
Fe	0.40	0.53

Back matter: Extra things unrelated to the project.

We can also conclude, that the capping layer was a Handy-cap.